SINGLE WALL CARBON NANOTUBE-POLYMER SOLAR CELLS

Sheila G. Bailey
NASA Glenn Research Center, Cleveland, OH 44135, USA

Stephanie L. Castro
Ohio Aerospace Institute, Brookpark, OH 44142, USA

Brian J. Landi, Thomas Gennett, and Ryne P. Raffaelle
NanoPower Research Laboratories, Rochester Institute of Technology, Rochester, NY 14623, USA

Investigation of single wall carbon nanotube (SWNT)-polymer solar cells has been conducted towards developing alternative lightweight, flexible devices for space power applications. Photovoltaic devices were constructed with regioregular poly(3-octylthiophene)-(P3OT) and purified, >95% w/w, laser-generated SWNTs. The P3OT composites were deposited on ITO-coated polyethylene terapthalate (PET) and I-V characterization was performed under simulated AM0 illumination. Fabricated devices for the 1.0% w/w SWNT-P3OT composites showed a photoresponse with an open-circuit voltage (V_{oc}) of 0.98 V and a short-circuit current density (I_{sc}) of 0.12 mA/cm^2. Optimization of carrier transport within these novel photovoltaic systems is proposed, specifically development of nanostructure-SWNT complexes to enhance exciton dissociation.

INTRODUCTION

The lure of large area, inexpensive, and environmentally benign solar cells has attracted many researchers over the past four decades or so. Since the early 1990's, considerable attention has turned to lightweight, flexible organic thin-film photovoltaics based on soluble conducting polymers.[1] This new class of devices relies upon the interaction between a nanomaterial and a conjugated polymer.[2] In addition to enhancing photovoltaic conversion efficiency, the incorporation of nanomaterials can potentially improve photochemical, mechanical, and environmental stability.

Photon absorption in the organic based composites produces bound-state excitons. Dissociation of these charge pairs can be accomplished by the potential difference across a polymer-metal junction provided the excitons are near the interface. However, the dissociation can also be accomplished via electron accepting impurities.[2] Thus, under illumination a preferential transfer of electrons to the acceptors will leave holes to be preferentially transported through the conjugated polymer. This process is known as photoinduced charge transfer. Since the discovery of photoinduced charge transfer, a variety of acceptor materials have been introduced into donating conjugated polymers to produce photovoltaic devices (i.e., Buckminster fullerenes,[3,4] CdSe quantum dots and nanorods,[5] and single wall carbon nanotubes[6]). Typical devices are produced by placing the doped polymeric films between a transparent conductive oxide (TCO) top contact and a metallic back contact.

The use of SWNTS in this type of device is a particularly attractive approach for several reasons. The extremely high surface area, ~1600 m^2/g reported for purified SWNTs,[7] offers a tremendous opportunity for exciton dissociation. Since SWNTs have diameters of ~1 nm and lengths on the order of microns, these materials exhibit significantly large aspect ratios (>10^3). At low doping levels, percolation pathways are established providing the means for a high carrier mobility and efficient charge transfer. This has been a problem in the majority of polymer solar cells developed to date, even with the advent of semiconductor nanorods. Since the diffusion distances for excitons in conducting polymers, poly(phenylenevinylene) for example, have been reported at <10 nm,[4] the requirement for a sufficient percolation network of electron-accepting dopants in the polymer composite is substantiated. Electrical conductivity data has validated that SWNT-doped polymer composites demonstrate this extremely low

percolation threshold. For SWNT-epoxy composites, the electrical conductivity has been claimed to rise by nearly 10^5 S/cm between 0.1 and 0.2% w/w loading.[8]

Other beneficial properties of SWNTs relevant to polymeric photovoltaic development include composite reinforcement and thermal management. Single wall carbon nanotubes have shown promise in the development of polymer composites with enhanced mechanical strength by load transfer from the polymer matrix to the dopant.[9] Tensile strengths for SWNTs have been estimated to equal ~20 GPa,[10] while the Young's modulus measured by atomic force microscopy is ~1 TPa.[11] This high Young's modulus and strength-to-weight ratio could help provide much needed mechanical stability to large area thin-film arrays. Single wall carbon nanotubes may also provide assistance in thermal management for such arrays. The thermal conductivity of an isolated (10, 10) SWNT has been theoretically predicted to be as high as 6600 W/mK.[12] Polymer composites doped with as little as 1% w/w SWNTs have shown a 70% increase in the thermal conductivity at 40 K.[8]

The viability of incorporating SWNTs into a conducting polymer for photovoltaic devices was established in 2002, utilizing arc-generated SWNT- poly(3-octylthiophene)-(P3OT) composites.[6] Their results showed a diode response for devices constructed in the sandwich formation, containing the composite film between an indium-tin-oxide (ITO) front contact and aluminum back contact. There was a photoresponse under AM1.5 illumination for both the pristine P3OT device and a 1% SWNT-P3OT composite blend, albeit the composite exhibits current densities several orders of magnitude higher. The photoresponse for a 1% w/w doped SWNT-P3OT composite was reported to have an open-circuit voltage (V_{oc}) of 0.75 V and a short-circuit current density (I_{sc}) of 0.12 mA/cm^2, in comparison to a V_{oc}= 0.35 V and I_{sc}= 0.7 μA/cm^2, for the pristine P3OT device.[6]

Originally, the SWNT-P3OT cells were described using the metal-insulator-metal (MIM) model for determining the V_{oc} based on a work function differential between the two metal electrodes. In the reported case, the maximum V_{oc} would be ~0.4 V based on values of 4.3 eV for Al and 4.7 eV for ITO,[6] although work has been done to show some variability in the work function of ITO dependent on processing and oxygen content.[13] Recent work has shown that investigation of differing work function metal electrodes that the MIM model is not applicable for SWNT-P3OT systems, due to a consistent V_{oc} of 0.75V. Rather, they propose that internal SWNT/polymer junctions based on the highest occupied molecular orbital (HOMO)-lowest unoccupied molecular orbital (LUMO) of the respective materials leads to enhanced charge separation and collection, providing the higher observed V_{oc} value.[14] In principle, control over these junctions may be garnered by reducing defect sites, altering the diameter distributions (which is inversely related to the bandgap in semiconducting types), or varying the concentration ratio of metallic to semiconducting for the SWNTs prior to dispersion. Such processing control offered by alternative synthesis conditions and purification strategies may further improve the V_{oc} and in turn produce more efficient SWNT-polymer solar cells.

EXPERIMENTAL

Single wall carbon nanotubes used for this study were synthesized using the pulse laser vaporization technique, employing an Alexandrite laser (755 nm) which pulsed the surface of a 0.6 at.% Ni/Co doped graphite target at a power density of 20 - 150 W/cm^2. The reaction furnace temperature was held at 1150°C, while the chamber was at a pressure of 400 torr with 100 sccm flowing $Ar_{(g)}$.[15] The as-produced SWNTs were collected from the condensed region on the quartz tube outside the furnace and purified by modification of the previously reported procedure.[16] In short, ~50 mg of as-produced SWNTs were refluxed in 3M nitric acid for 16 hours, and then filtered over a 0.2 μm PTFE membrane filter with copious amounts of de-ionized water. After drying the membrane filter at 70°C in vacuo to remove the SWNT paper, thermal oxidation proceeded in air at 500°C for one hour in a muffle furnace. Use of a 6M Hydrochloric acid wash for one hour in a water bath sonicator was at times necessary to remove any remaining metal catalyst impurities, with similar filtering steps. Finally, thermal oxidation at 550°C in air for one hour completed the purification. Raman spectroscopy, surface area analysis, scanning electron microscopy (SEM), optical absorption spectroscopy, and thermal gravimetric analysis (TGA) were utilized to fully characterize all raw soot and purified materials.

Preparation of the SWNT-P3OT composite solutions was performed using a series of mixing and sonication steps as previously demonstrated for other SWNT-polymer systems.[17] The necessary amount of regioregular P3OT, supplied by Aldrich, was dissolved in chloroform using water bath sonication to achieve the pristine 15 mg/mL solution. Composite dispersion was performed by

combining the appropriate mass of purified SWNTs to the pristine solution at desired doping levels. The composite solution was then placed in a water bath sonicator for five minutes prior to high speed stirring at room temperature for 72 hours. Aliquots of this dispersed solution were cast on Teflon substrates at room temperature to produce desired thin films required for optical absorption spectroscopy.

Device fabrication involved the use of commercially-obtained, high quality (i.e., < 10 Ω/sq.) ITO-coated polyethylene terapthalate (PET) substrates. The required cleaning of the ITO substrate prior to deposition was performed by sonication and rinsing of cut samples (1 inch x 1.5 inches) in de-ionized water, acetone, and methanol. Initially, an intrinsic layer of pristine P3OT is spray deposited (~1-2 mL of the 15 mg/mL solution) onto the masked, 1 $in.^2$ active area of the substrate. This is followed with spray deposition of the SWNT-P3OT composite solutions at similar volumes. As seen in Figure 1, completion of the solar cell occurs when aluminum contacts (typical thicknesses of 1000Å) are applied to the ITO and SWNT-P3OT composite film layers. This is accomplished using thermal evaporation under vacuum at pressures $<10^{-6}$ mbar with a standard shadow mask.

Solar cell testing was performed in an isolated black box configuration to assure standard calibration and reproducibility of results. Thin film SWNT-P3OT cells were placed on a temperature-controlled stage, held at 20ºC, during analysis. The I-V characteristics were monitored using a Keithley 237 source measurement unit. Simulated AM0 illumination was achieved by calibration of ELH lamps with a NASA certified Si standard cell.

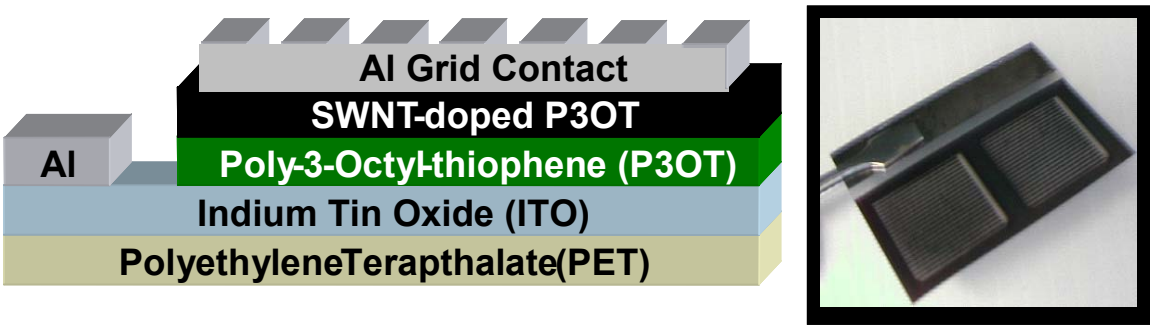

(a) (b)

Figure 1. (a) Schematic representation and (b) image depicting the composition of fabricated SWNT-P3OT flexible solar cells

RESULTS

The ability to elicit control over as-produced SWNTs is a major advantage for using pulse laser vaporization synthesis techniques. Such parameters as diameter distribution, defect density, and metallic to semiconducting ratios can be altered based on the synthesis conditions.[15,16,18] The as-produced SWNTs used in this study were synthesized and purified under typical conditions, where substantial yields and minimal defects have been observed. Shown in Figure 2 is a representative (a) SEM image of purified, >95% w/w SWNTs, and (b) an overlay of the Raman spectra for the radial breathing mode (RBM) of this sample for incident laser energies of 1.96 and 2.55 eV. The SEM image shows an entangled "mat" of SWNTs with no significant metal catalyst impurities or amorphous carbon coatings. The high purity SWNTs will "bundle" due to the Van der Waals interaction between the individual tubes. Control over the influence of bundling can potentially be addressed through polymeric interaction. Previous work has suggested a "debundling" effect with SWNT-Nafion composites, observed by SEM, that was proposed to reduce the necessary doping level for a percolation threshold.[17] Dispersions of SWNTs in P3OT may follow similar results, although full evaluation of this has not yet been performed. In addition, Raman spectroscopy can be used to determine the diameter distribution, chirality, and defect density of the as-produced and purified SWNTs. The RBM is routinely used to

calculate the diameter distribution.[19] Using two incident laser energies during analysis allows for the determination of SWNT type, i.e. semiconducting vs. metallic.[20,21] For this diameter range, the 1.96 eV laser resonantly enhances predominantly metallic SWNTs which correspond to ~1.2-1.4 nm in diameter.[19] Similarly, the 2.55 eV laser probes the semiconducting type, also shown to contain equivalent diameters for the purified sample.

The homogeneous distribution of SWNTs in a polymer matrix is dependent upon the ability of the polymer chain to associate with the SWNT superstructure. Stable composite dispersions of 0.1% and 1.0% w/w SWNTs in P3OT were produced and analyzed in this study. Optical spectroscopy was conducted to observe the SWNT doping level effects on the absorption properties and infer potential electronic interactions between dopant and polymer.

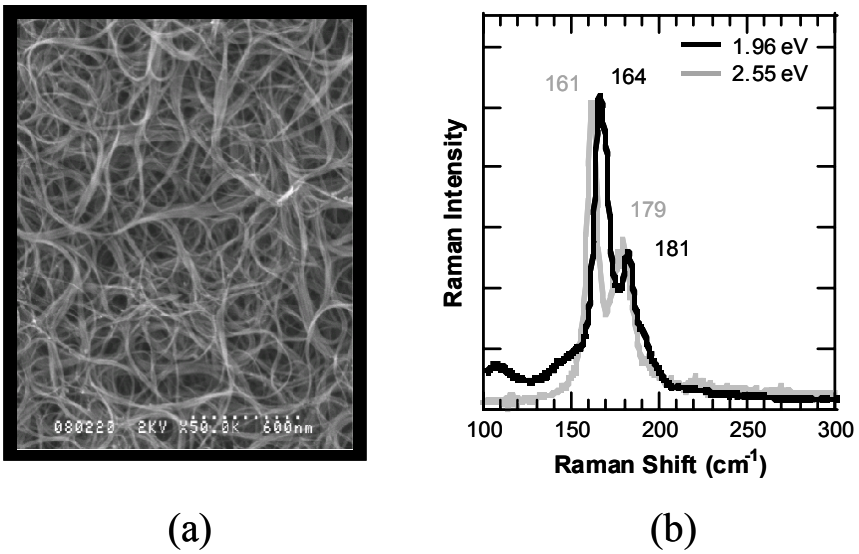

Figure 2. (a) SEM image of purified, >95% w/w SWNTs, and (b) overlay of Raman spectrum for the RBM of (a) at incident laser energies of 1.96 and 2.55 eV. The labeled peaks correspond to a diameter distribution between 1.2-1.4 nm for both metallic and semiconducting SWNTs.

Shown in Figure 3 is an overlay of these spectra where the pristine P3OT shows strong optical absorption at energies >2 eV. As expected, variation in absorption properties for the SWNT-P3OT composites is observed as the doping level increases. Through modification of the SWNT doping level in the polymer, it is possible to alter the absorption pattern of these composite materials. In fact, at these relatively low doping levels, the P3OT shows a significant enhancement in absorption through the near-IR and visible regions. The gray curve for purified SWNTs is offset from the other three for clarity, but indicates the typical complex pattern observed for this spectral range. The two lowest energy peaks for SWNTs (~0.7 eV and ~1.3 eV) are representative of the energy transitions corresponding to the 1st and 2nd Van Hove (VH) singularities for semiconducting types, respectively.[22] The SWNT-P3OT composites display a relative quenching of the 1st VH compared to the 2nd VH, which is typical of doping effects on the SWNTs.[23,24] Therefore, an apparent doping of the semiconducting SWNTs by the polymer is present. However, due to the higher intensity at larger energies, typical of absorption for the metallic SWNTs (~1.8 eV), any interaction between these SWNT types and the polymer is presently unavailable.

Application of SWNT-P3OT composite solutions to the constructed devices was performed using a solution-spray technique onto the ITO/PET substrates. The unique approach to deposit these photoactive composites on polymer substrates demonstrates the inherent advantages of thin film polymeric solar cells, namely low structural weight and flexibility. These novel polymeric solar cells were constructed for pristine P3OT, 0.1% w/w, and 1.0% w/w SWNTs in P3OT, and tested under simulated AM0 illumination to determine the respective I-V characteristics. The typical photoresponse observed for pristine P3OT and 1% w/w SWNT-P3OT cells is shown in Figure 4. Although each overlay

shows significant enhancement in both I_{sc} and V_{oc} upon illumination, there is an absense of the typical diode "knee" for both cases. The cause of the larger than expected reverse bias currents is presently not understood. This effect may be attributed to long-lived energy states for the SWNTs and P3OT or the presense of carrier traps which reduces the I_{sc}.

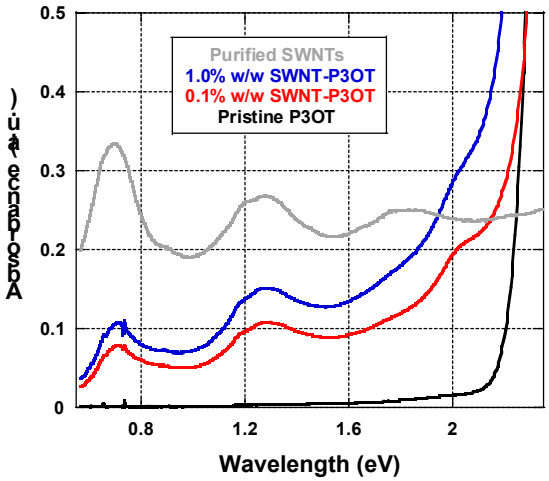

Figure 3. Optical absorption overlay for thin films of pristine P3OT (black), 0.1% w/w SWNT-P3OT composite (red), 1.0% w/w SWNT-P3OT composite (blue), and purified SWNTs (gray). Enhancement in absorption for the composites relative to the pristine P3OT is clearly observed

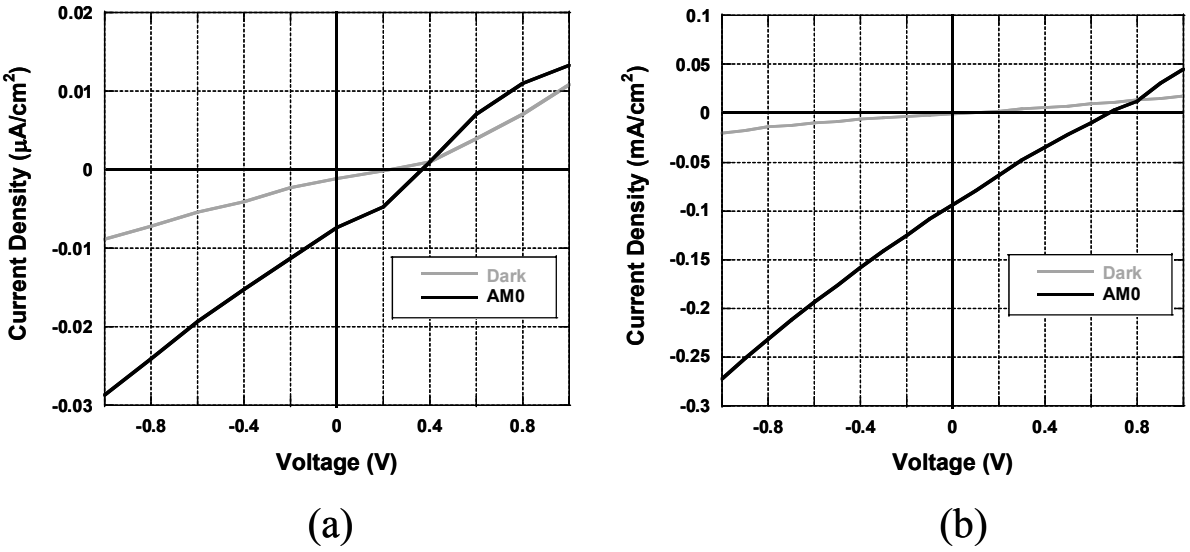

Figure 4. Characteristic I-V plots in the dark (gray) and under simulated AM0 illumination (black), displaying the photoresponse for (a) pristine P3OT and (b) 1% w/w SWNT-P3OT composite solar cells

Further characterization of the composite cells showed a corresponding increase in the I_{sc} as the doping level of SWNTs increased in the P3OT. Figure 5 shows an I-V overlay under the simulated AM0 illumination for the pristine P3OT, 0.1%, and 1.0 % w/w SWNT-P3OT cells in the region of forward bias. Clearly evident is an order of magnitude increase in the I_{sc} from the pristine P3OT to the 0.1% w/w SWNT-P3OT composite cell. An additional increase of ~50% is observed when the doping level reaches 1.0% w/w, with an I_{sc} equal to 0.12 mA/cm^2 for the cell. This result indicates that there is an apparent conductivity effect on the I_{sc} in the composite films which can be controlled by SWNT doping. Optimization of the doping level for maximum current density is a necessary step at improving the overall efficiency of these cells. Similarly, the V_{oc} more than doubled for both SWNT-doped cells,

although the 0.1% w/w composite has a slightly higher value than the 1.0 % w/w composite. Interestingly, the measured V_{oc} of 0.98 V is signficantly higher than the recent report, where they postulated that the energy difference in the HOMO-LUMO levels of the SWNT/polymer junction is responsible for the open-circuit-voltage.[14] An explanation of this current result may reside in the purity and defect density of the SWNTs. This is an important variable to consider since the interaction between SWNTs and the polymer can directly affect the junction by which exciton dissociation occurs. Other variables to evaluate for SWNT-polymer solar cells are the diameter distributions and metallic to semiconducting ratios of the dopant. If the SWNTs are primarily acting as a conductive network, then the presence of metallic types would be the preferential dopant. However, the possibility exists that semiconducting SWNTs are participating in the photoconversion process since a recent report has shown certain photoconductivity effects exist for SWNTs.[25] In either case, selective dispersion of one type could lead to higher SWNT-P3OT solar cell efficiencies. Above all though, the ability to dissociate and extract the generated carriers upon illumination in these conducting polymer solar cells is the foremost concern to augment the overall efficiency.

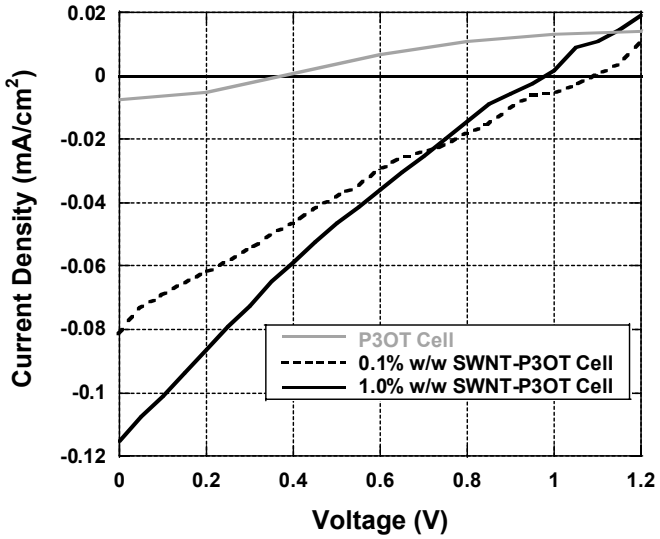

Figure 5. Overlay of the I-V relationship under simulated AM0 illumination for pristine P3OT (gray), 0.1% w/w SWNT-P3OT composite (black dashed), and 1.0% w/w SWNT-P3OT composite (black line) solar cells.

A next-generation approach to maximizing the charge separation and carrier transport in SWNT-doped P3OT cells may be through attachment of nanostructured components to the SWNTs (see Figure 6a). Such versatility enables tuning of the optoelectronic properties of the dopant in the polymer cell to match the energy bands between components and conducting polymer HOMO/LUMO levels. Our approach to improve device efficiency is through covalent attachment of semiconducting quantum dots to SWNTs. It is expected that conjugation of SWNTs and quantum dots prior to dispersion will facilitate charge dissociation and transport in the polymer solar cells. Our initial attempt at establishing the necessary chemistry has been successful with attachment of CdSe quantum dots to functionalized SWNTs through an ethylenediamine (en) linker, similar to the reported procedures.[26,27] Shown in Figure 6b is a tapping-mode atomic force micrograph (AFM) of our resulting CdSe-en-SWNT complexed sample. Incorporation of this material into similar P3OT composite solar cells as described here, is currently under investigation.

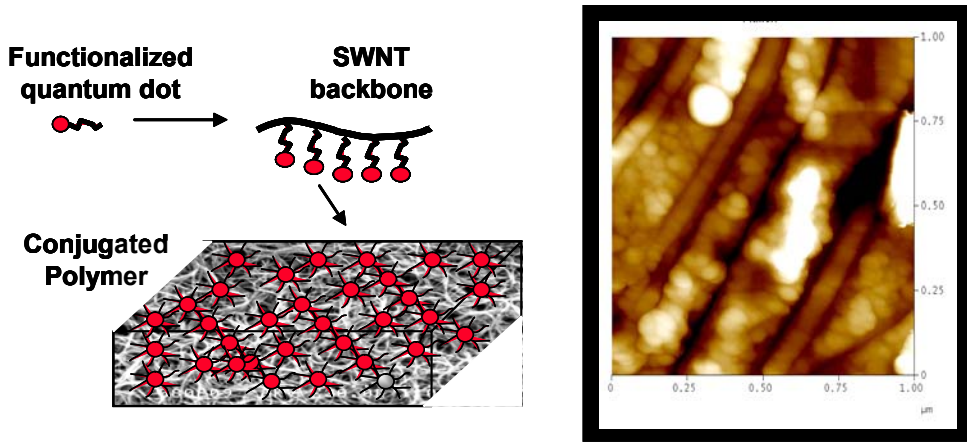

(a) (b)

Figure 6. (a) Schematic representation of the approach to conjugate quantum dots with SWNTs prior to dispersion in the conducting polymer; (b) AFM image of CdSe-en-SWNTs to be used as dopant in future SWNT-P3OT solar cells.

CONCLUSIONS

The ability to construct flexible solar cells containing SWNT doped polymer composites has been demonstrated. Devices containing 1% w/w SWNTs in P3OT have shown a photoresponse with low current densities but relatively high open-circuit voltages (~1 V). Attempts to improve the exciton dissociation and carrier transport in these systems may rely upon controlled processing of SWNTs for appropriate material properties. Ultimately, the ability to covalently attach other nanomaterials to the SWNTs could result in higher polymer solar cell efficiencies.

ACKNOWLEDGEMENTS

This work was supported by NASA Glenn Research Center through grant NAG3-2595 and the National Science Foundation through grant ECS 0233776. The authors wish to thank Stephen Fahey for obtaining the AFM images.

REFERENCES

(1) Yu, G.; Gao, J.; Hummelen, J. C.; Wudl, F.; Heeger, A. J. *Science* **1995**, *270*, 1789-1791.
(2) Granstrom, M.; Petritsch, K.; Arias, A. C.; Lux, A.; Andersson, M. R.; Friend, R. H. *Nature* **1998**, *395*, 257-360.
(3) Camaioni, N.; Ridolfi, G.; Casalbore-Miceli, G.; Possamai, G.; Garlaschelli, L.; Maggini, M. *Solar Energy Materials & Solar Cells* **2002**.
(4) Halls, J. J. M.; Pichler, K.; Friend, R. H.; Moratti, S. C.; Holmes, A. B. *Appl. Phys. Lett.* **1996**, *68*, 3120-3122.
(5) Huynh, W. U.; Dittmer, J. J.; Alivisatos, A. P. *Science* **2002**, *295*, 2425-2427.
(6) Kymakis, E.; Amaratunga, G. A. J. *Appl. Phys. Lett.* **2002**, *80*, 112-114.
(7) Cinke, M.; Li, J.; Chen, B.; Cassell, A.; Delzeit, L.; Han, J.; Meyyappan, M. *Chem. Phys. Lett.* **2002**, *365*, 69.
(8) Biercuk, M. J., Llaguno, M.C., Radosavljevic, M., Hyun, J.K., Johnson, A.T., Fischer, J.E. *Appl. Phys. Lett.* **2002**, *80*, 2767-2769.
(9) Schadler, L. S.; Giannaris, S. C.; Ajayan, P. M. *Appl. Phys. Lett.* **1998**, *73*, 3842.
(10) Li, F., Cheng, H.M.; Bai, S.; Su, G.; Dresselhaus, M.S. *Appl. Phys. Lett.* **2000**, *77*, 3161-3163.
(11) Salvetat, J.; Briggs, G. A. D.; Bonard, J.; Bacsa, R. R.; Kulik, A. J.; Stockli, T.; Burnham, N. A.; Forro, L. *Phys. Rev. Lett.* **1999**, *82*, 944.

(12) Berber, S.; Kwon, Y.; Tomanek, D. *Phys. Rev. Lett.* **2000**, *84*, 4613.
(13) Sugiyama, K.; Ishii, H.; Ouchi, Y.; Seki, K. *J. Appl. Phys.* **2000**, *87*, 295.
(14) Kymakis, E.; Alexandrou, I.; Amaratunga, G. A. J. *J. Appl. Phys.* **2003**, *93*, 1764.
(15) Gennett, T.; Dillon, A. C.; Alleman, J. L.; Jones, K. M.; Parilla, P. A.; Heben, M. J. *Mat. Res. Soc. Symp. Proc.* **2001**, *633*, A2.3.1.
(16) Dillon, A. C.; Gennett, T.; Jones, K. M.; Alleman, J. L.; Parilla, P. A.; Heben, M. J. *Adv. Mater.* **1999**, *11*, 1354.
(17) Landi, B. J.; Raffaelle, R. P.; Heben, M. J.; Alleman, J. L.; VanDerveer, W.; Gennett, T. *Nano Lett.* **2002**, *2*, 1329.
(18) Dillon, A. C.; Parilla, P. A.; Alleman, J. L.; Perkins, J. D.; Heben, M. J. *Chem. Phys. Lett.* **2000**, *316*, 13.
(19) Rao, A. M.; Chen, J.; Richter, E.; Schlecht, U.; Eklund, P. C.; Haddon, R. C.; Venkateswaran, U. D.; Kwon, Y. K.; Tomanek, D. *Phys. Rev. Lett.* **2001**, *86*, 3895.
(20) Alvarez, L.; Righi, A.; Guillard, T.; Rols, S.; Anglaret, E.; Laplaze, D.; Sauvajol, J. L. *Chem. Phys. Lett.* **2000**, *316*, 186.
(21) Dresselhaus, M. S.; Dresselhaus, G.; Jorio, A.; Souza Filho, A. G.; Saito, R. *Carbon* **2002**, *40*, 2043.
(22) Kataura, H.; Kumazawa, Y.; Maniwa, Y.; Umezu, I.; Suzuki, S.; Ohtsuka, Y.; Achiba, Y. *Synth. Met.* **1999**, *103*, 2555.
(23) Minami, N.; Kazaoui, S.; Jacquemin, R.; Yamawaki, H.; Aoki, K.; Kataura, H.; Achiba, Y. *Synth. Met.* **2001**, *116*, 405.
(24) Kazaoui, S.; Minami, N.; Kataura, H.; Achiba, Y. *Synth. Met.* **2001**, *121*, 1201.
(25) Freitag, M.; Martin, Y.; Misewich, J. A.; Martel, R.; Avouris, P. *Nano Lett.* **2003**, *3*, 1067.
(26) Banerjee, S.; Wong, S. S. *Nano Lett.* **2002**, *2*, 195-200.
(27) Haremza, J. M.; Hahn, M. A.; Krauss, T. D.; Chen, S.; Calcines, J. *Nano Lett.* **2002**, *2*, 1253.